Cathepsin K-sensitive poly(ethylene glycol) hydrogels for degradation in response to bone resorption

Chih-Wei Hsu,[1]* Ronke M. Olabisi,[1]* Elizabeth A. Olmsted-Davis,[2] Alan R. Davis,[2] Jennifer L. West[1]

[1]Department of Bioengineering, Rice University, 6100 Main St., Houston, Texas 77005
[2]Center for Cell and Gene Therapy, Baylor College of Medicine, One Baylor Plaza, Houston, Texas 77030

Received 1 September 2010; revised 10 January 2011; accepted 31 January 2011
Published online 26 April 2011 in Wiley Online Library (wileyonlinelibrary.com). DOI: 10.1002/jbm.a.33076

Abstract: We propose a new strategy of biomaterial design to achieve selective cellular degradation by the incorporation of cathepsin K-degradable peptide sequences into a scaffold structure so that scaffold biodegradation can be induced at the end of the bone formation process. Poly(ethylene glycol) diacrylate (PEGDA) hydrogels were used as a model biomaterial system in this study. A cathepsin K-sensitive peptide, GGGMGPSGPWGGK (GPSG), was synthesized and modified with acryloyl-PEG-succinimidyl carbonate to produce a cross-linkable cathepsin K-sensitive polymer that can be used to form a hydrogel. Specificity of degradation of the GPSG hydrogels was tested with cathepsin K and proteinase K as a positive control, with both resulting in significant degradation compared to incubation with nonspecific collagenases over a 24-h time period. No degradation was observed when the hydrogels were incubated with plasmin or control buffers. Cell-induced degradation was evaluated by seeding differentiated MC3T3-E1 osteoblasts and RAW264.7 osteoclasts on GPSG hydrogels that were also modified with the cell adhesion peptide RGDS. Resulting surface features and resorption pits were analyzed by differential interference contrast (DIC) and fluorescent images obtained with confocal microscopy. Results from both analyses demonstrated that GPSG hydrogels can be degraded specifically in response to osteoclast attachment but not in response to osteoblasts. In summary, we have demonstrated that by incorporating a cathepsin K-sensitive peptide into a synthetic polymer structure, we can generate biomaterials that specifically respond to cues from the natural process of bone remodeling. J Biomed Mater Res Part A: 98A: 53–62, 2011.

Key Words: hydrogel, biodegradation, bone remodeling, osteoclast

INTRODUCTION

Autologous bone grafts are considered the gold standard treatment in orthopedic surgery, where the biological properties of the grafts can undergo balanced bone formation and bone resorption at the implanted sites. These grafts have been commonly used in spinal fusion, revision total hip arthroplasty, maxillofacial reconstruction, and repair of segmental skeletal defects.[1–4] Despite being the standard of care, autografts are limited by donor-site morbidity and availability. As an alternative to the bone graft, three main classes of biomaterial have been designed and used extensively for different orthopedic applications: metals, ceramics, and polymers.[5] Although each class of biomaterial has its own advantages, poor degradation properties are a major drawback common to all. At best, these materials undergo nonspecific degradation, and at worst, they are essentially nondegradable.

The ideal biomaterial for orthopedic applications should be osteoconductive, osteoinductive, osteogenic, and also bioresorbable. An important aspect of designing a degradable biomaterial for orthopedic applications is the ability to synchronize the degradation of the material with cellular responses that occur during bone remodeling—a dynamic process consisting of both bone formation and resorption.[6] Bone formation is accomplished following mineralization by matrix producing osteoblasts, whereas bone resorption is carried out by osteoclasts. When the resorption cycle starts, osteoclasts migrate and attach to resorption sites. Attached osteoclasts then polarize and the apex membrane forms a functional secretory domain. Polarized osteoclasts secrete hydrochloric acid to dissolve hydroxyapatite and proteases to degrade the type I collagen-rich organic matrix. One such protease is cathepsin K, which is predominantly expressed in osteoclasts during bone resorption.[7,8] In the current study, by incorporating a collagen I (α-1) peptide fragment, we have developed a synthetic polymer with high sensitivity and specificity for cathepsin K.

Herein we describe such a biomaterial that was designed using our new strategy for creating biodegradable materials that degrade in response to specific cellular events. With poly(ethylene glycol) diacrylate (PEGDA) hydrogels as a model system, we demonstrate that we can fabricate

Additional Supporting Information may be found in the online version of this article.
*These authors contributed equally to this work.
Correspondence to: J. L. West; e-mail: jwest@rice.edu
Contract grant sponsor: Department of Defense; contract grant number: W82XWH-04-1-0068

the hydrogel scaffold to be gradually degraded and specifically targeted by bone resorption processes. The degradable hydrogel is designed by incorporating a short peptide fragment of type I collagen (α-1), (160-163), Gly-Pro-Ser-Gly (GPSG), which was found to be highly cleavable between serine and glycine by cathepsin K.[9] After inserting this peptide into a PEGDA backbone, we evaluated the degradation profiles of the cathepsin K-sensitive GPSG hydrogel in the presence of select enzymes. We also examined the hydrogel's capacity for degradation by osteoclasts and osteoblasts.

MATERIALS AND METHODS

Specificity of degradation of the cathepsin K-sensitive peptide

The cathepsin K-sensitive peptide sequence, GPMGPSGP WGK, and a scrambled sequence, GMPSGGPPWGK, were synthesized on an APEX 396 peptide synthesizer (Aapptec, Louisville, KY). After synthesis, the peptides were cleaved from the polystyrene resin (95% trifluoroacetic acid, 2.5% water, and 2.5% triisopropylsilane), precipitated in ethyl ether, and purified by dialysis. Following purification, the peptide molecular weights were confirmed with matrix-assisted laser desorption ionization time of flight mass spectrometry (MALDI-ToF; Bruker Daltonics, Billerica, MA).

Degradation products of these peptides were evaluated by MALDI-ToF after incubation with cathepsin K or a control solution. Procathepsin K (Enzo Life Science, Plymouth Meeting, PA) was first activated in 35 m*M* sodium acetate (pH 3.5) for 2 h at room temperature. Activated cathepsin K was then adjusted to 0.05 mg/mL in 50 m*M* sodium acetate buffer (NaOAc; pH 5.5, 2.5 m*M* EDTA, 1 m*M* DTT, 0.01% Triton X-100, 0.2 mg/mL sodium azide). NaOAc buffer without enzyme was used as a negative control and the reactions were allowed to proceed for 4 h at 37°C. The molecular weights of the degradation products were determined with MALDI-ToF mass spectrometry.

Synthesis and characterization of acryloyl-PEG-succinimidyl carbonate (acrylol-PEG-SMC)

All reagents were obtained from Sigma unless otherwise noted. Monoacrylation of poly(ethylene glycol) (PEG) was undertaken by reacting the PEG with a stoichiometric amount of acryloyl chloride in the presence of silver(I) oxide and a catalytic amount of potassium iodide, a process shown to selectively monofunctionalize PEG in high yields due to intramolecular hydrogen bonding between the two hydroxyl groups, which differ in acidity.[10] After reacting PEG (50 m*M*; 3400 Da; Fluka, Milwaukee, WI) with 1.5 molar equivalent silver(I) oxide (75 m*M*), 1.1 molar equivalent acryloyl chloride (55 m*M*) and potassium iodide (30 m*M*) in anhydrous dichloromethane (DCM) overnight at 4°C, the mixture was purified. Silver(I) oxide was first removed from the acryloyl-PEG-OH solution by filtering the mixture through a Celite 521 pad (Spectrum Chemical Manufacturing Corp, Gardena, CA). For further purification, the filtrate was dried using a Rotovap, re-dissolved in de-ionized water, and adjusted to pH 3 with 6*N* HCl. After heating to 35°C and venting to air for 1 h, activated charcoal (Fisher Scientific, Pittsburgh, PA) was added to the mixture and stirred overnight to absorb iodine. The charcoal was then removed via filtration. Sodium chloride (25% w/v) was dissolved in the aqueous filtrate followed by DCM extraction. The organic phase was collected and extracted again with 2*M* potassium bicarbonate to remove chloride ions. Acryloyl-PEG-OH was recovered by precipitation in cold ethyl ether, filtered, dried under vacuum overnight, and lyophilized until completely dry. To proceed with the succinimidyl carbonate conjugation, acryloyl-PEG-OH (25 m*M*) was mixed with pyridine (75 m*M*) and *N,N′*-disuccinimidyl carbonate (100 m*M*) in anhydrous acetonitrile. After reacting under argon overnight, pyridine and acetonitrile were removed with a Rotovap. The mixture was re-dissolved in anhydrous DCM and filtered to remove unreacted *N,N′*-disuccinimidyl carbonate. Acetate buffer (0.1*M*, pH 4.5, 15% NaCl) was then used for phase extraction. The organic layer was collected and dried with anhydrous magnesium sulfate. Acryloyl-PEG-SMC [Fig. 1(A)] was recovered following precipitation in cold ethyl ether, filtered, and dried under vacuum overnight. The products were analyzed by ^{1}H NMR (Advance 400, Bruker, Germany) and MALDI-ToF and stored at −80°C under argon.

Synthesis and characterization of acryloyl-PEG-GPSG-PEG-acryloyl, acryloyl-PEG-RGDS, and fluorescently-labeled acryloyl-PEG-RGDS conjugates

The cathepsin K-sensitive peptide sequence GGGMGPSGP WGGK (GPSG) was synthesized on an APEX 396 peptide synthesizer and purified as previously described. The glycine spacers sandwiching the peptide were included to avoid steric hindrance with cathepsin K following conjugation to PEG. Lysine, with a free amine on its side chain, enabled reaction with the active esters in the heterobifunctional acryloyl-PEG-SMC. The tryptophan residue allows the tracking of *in vitro* degradation by monitoring UV absorbance at 280 nm as the cleaved amino acid is released to solution.

The crosslinkable cathepsin K-sensitive acryloyl-PEG-GGGMGPSGPWGGK-PEG-acryloyl (acryloyl-PEG-GPSG-PEG-acryloyl) polymer was synthesized by reacting the GPSG peptide with acryloyl-PEG-SMC in a 2.1:1 (PEG:peptide) molar ratio in a 50 m*M* sodium bicarbonate buffer (pH 8.5) at room temperature overnight [Fig. 1(B)]. The resulting product was dialyzed, lyophilized, and stored under argon at −20°C until use. Similarly, the cell adhesive peptide Arg-Gly-Asp-Ser (RGDS, American Peptide, Sunnyvale, CA) was reacted with acryloyl-PEG-SMC in a 1.1:1 molar ratio to obtain acryloyl-PEG-RGDS. Conjugation products were analyzed by ^{1}H NMR, and gel permeation chromatography with UV/Vis and evaporative light scattering detectors (GPC, Polymer Laboratories, Amherst, MA).

Fluorescently labeled acryloyl-PEG-RGDS was synthesized as previously described.[11] In brief, purified acryloyl-PEG-RGDS was mixed with Alexa Fluor 680 carboxylic acid (Invitrogen, Carlsbad, CA) in 50 m*M* sodium bicarbonate buffer in a 1:10 (acryloyl-PEG-RGDS:dye) molar ratio and allowed to react for 1 h at room temperature. The desired products were then purified by a Sephadex G-25 fine chromatography column (Amersham Bioscience, Uppsala,

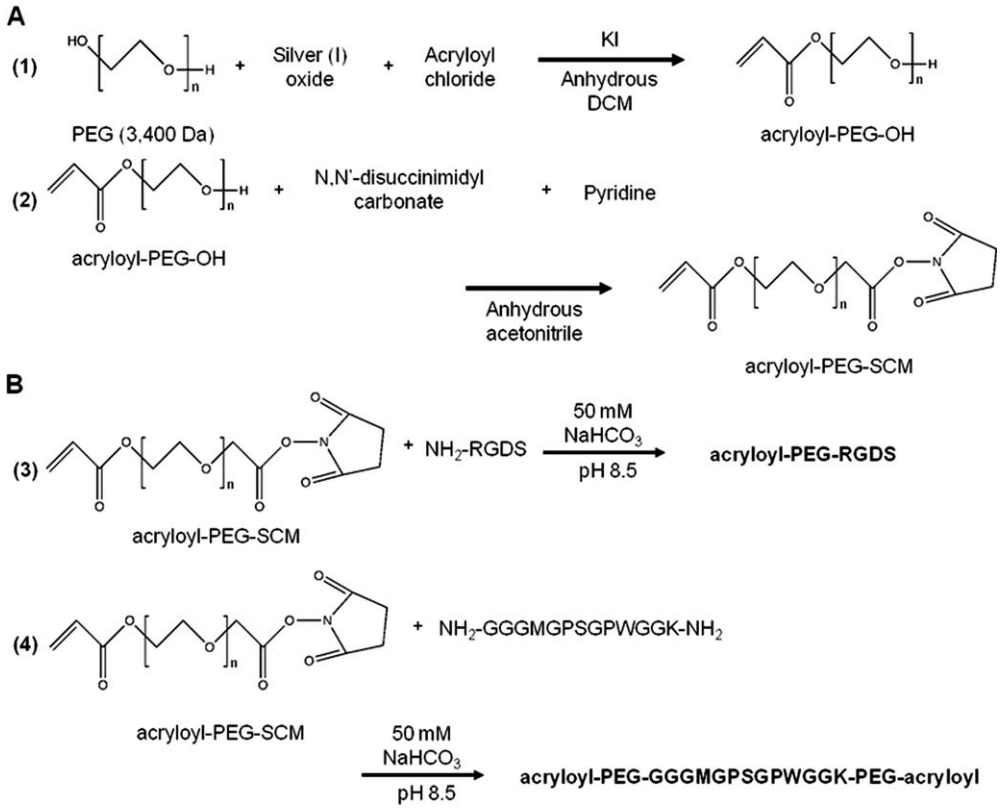

FIGURE 1. (A) Synthesis of acryloyl-PEG-succinimidyl carbonate (acryloyl-PEG-SCM) and (B) modification of PEG derivatives. The reaction of 3400 Da PEG first proceeded with (1) monoacrylation to produce acryloyl-PEG-OH. Monoacrylated PEG-OH was reacted with *N,N'*-disuccinimidyl carbonate to produce acryloyl-PEG-SCM. (2) Acryloyl-PEG-SCM was then reacted with the adhesive ligand RGDS to form acryloyl-PEG-RGDS (3) or reacted with the cathepsin K-sensitive peptide GGGMGPSGPWGGK to form a crosslinkable, cathepsin K-sensitive GPSG polymer (4).

Sweden) followed by dialysis and lyophilization. Recovered products were stored under argon at −20°C until use.

In vitro degradation profile of the PEG-GPSG-PEG hydrogel

For evaluation of PEG-GPSG-PEG hydrogel degradation, a prepolymer solution was prepared by combining 0.1 g/mL crosslinkable acryloyl-PEG-GPSG-PEG-acryloyl with 1.5% (v/v) triethanolamine, 37 m*M* 1-vinyl-2-pyrrolidinone, and 1% (v/v) of 1.0 m*M* eosin Y in tris buffered saline (TBS; pH 7.5, 10 m*M* $CaCl_2$, 0.1% Tween 20, 0.2 mg/mL sodium azide). The precursor solution was sterilized by filtration using a 0.22-μm filter (Millpore Corporation Bedford, MA). For *in vitro* enzyme degradation tests, 3 μL of the prepolymer solution was transferred to the bottom corner of a micro-cuvette (Brandtech, Essex, CT) and polymerized by exposing to visible light for 2 min. The power of the light source (Fiber Lite; Dolan Jenner Industries, Boxborough, MA) is 408 mW/cm^2 when measured at 490 nm, which is the excitation wavelength for Eosin Y. The spot temperature was measured to change in 2 min from 22°C to 29°C, well under the 37°C of the incubator. Following equilibrium swelling overnight in 250 μL TBS, each hydrogel was incubated with 250 μL enzyme solution at 37°C for 24 h. Proteinase K (Invitrogen), plasmin, type I and type III collagenase (COL I and COL III; Worthington, Lakewood, NJ) were prepared in TBS to final concentrations of 0.05 mg/mL. Hydrogels were also incubated in TBS and NaOAc buffer as negative controls. Hydrogel degradation was evaluated by monitoring the release of tryptophan over time by measuring the absorbance change of test solutions with a UV/Vis spectrophotometer (Carey 50, Varian, Palo Alto, CA) at 280 nm. The percentage released was calculated by comparing hydrogel degradation against an equivalent volume of uncrosslinked prepolymer solution after incubation with each respective enzyme. This control solution corresponds to 100% degradation.

Maintenance of MC3T3-E1 and RAW 264.7 cells

Murine preosteoblast cells MC3T3-E1 subclone 4 and macrophage cells RAW 264.7 (ATCC, Manassas, VA) were cultured in alpha-MEM medium (Gibco BRL, Canada) and DMEM (ATCC), respectively. Culture media were supplemented with 10% fetal bovine serum (FBS; Atlanta Biologicals, Lawrenceville, GA), 100 U/mL penicillin, and 100 mg/mL streptomycin (Gibco BRL, Canada). Cells were incubated at 37°C with 5% CO_2. The media were refreshed every two to three days and confluent cells were subcultured through trypsinization for MC3T3-E1 and scraping for RAW 264.7. All experiments were conducted using cells between passages 4 and 10. MC3T3-E1 cells were differentiated into osteoblasts via supplied 50 μg/mL ascorbic acid and 10 m*M* b-glycerophosphate to the growth medium. Differentiation medium was subsequently replaced every two to three days. To differentiate cells to multinuclear osteoclasts, RAW 264.7

were seeded at a density of 1.5×10^5 cells/cm^2 and allowed to adhere for 4 h. Culture media was then supplemented with 30 ng/mL of receptor activator of nuclear factor kappa B ligand (RANKL; R&D Systems Inc., Minneapolis, MN) and replaced every 2 days. The cells were cultured for an additional 4 days before further use.[12]

Serum gradient purification of differentiated multinuclear RAW264.7

Differentiated multinuclear RAW264.7 (dRAW264.7) were purified by a serum gradient.[12] After differentiation in culture medium supplemented with 30 ng/mL RANKL for 4 days, dRAW264.7 cells were trypsinized and resuspended in 15 mL of Moscona's high carbonate (MHB; pH 7.2, 137 m*M* NaCl, 2.7 m*M* KCl, 0.4 m*M* NaH_2PO_4, 12 m*M* $NaHCO_3$, and 11 m*M* dextrose) solution. A serum gradient was prepared by placing a layer of 15 mL 70% FBS solution in MHB at the bottom of a 50-mL conical tube, and slowly overlaying with a second layer of 15 mL 40% FBS solution. Fifteen milliliter of cell suspension was then slowly added to the top without disturbing the layers. The tube was capped and held undisturbed at room temperature for 30 min to permit cells to separate based on size. The top 17-mL layer, middle 16-mL layer, and bottom 12-mL layer were collected separately. Cells in each layer were centrifuged at $500 \times g$ for 5 min, resuspended in culture medium, and seeded in 12-well tissue culture plates at a density of 5000 cells/cm^2 overnight.

To confirm the presence of differentiated osteoclasts, cells were stained for the activity of tartrate-resistant acid phosphatase (TRAP) as previously described.[12] Briefly, after fixing cells in 4% formaldehyde, TRAP staining solution was prepared containing 0.125 mg/mL Naphthol AS-BI Phosphate, 0.1*M* acetate buffer, 6.7 m*M* L(+)-tartrate, 1 m*M* sodium nitrite, and 0.07 mg/mL diazotized fast garnet GBC. Medium was aspirated and 1 mL of TRAP staining solution was added to each well. After staining at 37°C for 1 h, each well was rinsed three times with deionized water and allowed to air dry before imaging.

Surface degradation of differentiated RAW 264.7 and MC3T3-E1 on PEG-GPSG-PEG hydrogels and bone

Flat hydrogel sheets for surface degradation studies were formed by adding 10 m*M* acryloyl-PEG-RGDS and 1 m*M* Alexaflour 680 labeled acryloyl-PEG-RGDS to the PEG-GPSG-PEG prepolymer mixture (0.1 g/mL acryloyl-PEG-GPSG-PEG-acryloyl with 1.5 % (v/v) triethanolamine, 37 m*M* 1-vinyl-2-pyrrolidinone, and 1% (v/v) of 1.0 m*M* eosin Y in TBS) and polymerizing between a mica sheet (Ted Pella, Inc., Redding, CA) and glass slide separated by a 1 mm Teflon spacer. The atomically smooth surface of the mica sheet permitted the formation of hydrogels with smooth surfaces that displayed no flaws even under high magnification. Both MC3T3-E1 and RAW 264.7 cells were differentiated for 4 days in differentiation media in tissue culture plates. dRAW264.7 cells were removed by scraping and reseeded at a density of 5×10^4 cells/cm^2 on both PEG-GPSG-PEG hydrogels and porcine cortical bone slices, which served as control. Differentiated MC3T3-E1 (dMC3T3-E1) and multinuclear RAW264.7 osteoclasts collected at the bottom layer of the serum gradient were also seeded on the mica-molded hydrogel surfaces at the same density. Hydrogels seeded with either osteoblasts or osteoclasts and bone slices seeded with osteoclasts were then cultured in differentiation medium for 48 h before further analysis.

Confocal microscopy of pit formation on cathepsin K-sensitive PEG hydrogel and bone surfaces

Following 48 h of incubation, hydrogel surfaces were imaged after cells were either removed by 20 m*M* EDTA, or fixed and stained with 4′,6-diamidino-2-phenylindole (DAPI; Invitrogen) and rhodamine phalloidin (Invitrogen). Similarly, bone slices were imaged following the removal of adherent dRAW264.7 cells. Differential interference contrast (DIC) or fluorescence images were taken using a LSM-5 LIVE microscope system (Carl Zeiss Inc., German). Z-stack images were acquired with a 20× objective. The z distance between each step was 0.253 μm. Images were all processed with ImageJ 142 (NIH, Bethesda, MD). Three dimensional image reconstructions were processed using OsiriX Medical Imaging software (version 3.0.2; the OsiriX Foundation, Geneva, Switzerland). The areas of resorption lacunae on hydrogel and bone surfaces were measured using ImageJ.

RESULTS

Characterization of synthesized materials

^{1}H NMR analysis demonstrated that acryloyl-PEG-SCM was successfully synthesized and conjugated to GGGMGPSGP WGGK and RGDS. After purification, the acryloyl-PEG-SCM showed the methylene protons of PEG as a triplet at 3.6–3.7 ppm, the succinimidyl carbonate protons at 2.6 ppm, as well as the acrylate protons at 5.9–6.4 ppm. After conjugation to GGGMGPSGPWGGK and RGDS, the peak for the succinimidyl carbonate protons disappeared, but peaks for the methylene protons of PEG and acrylate protons remained indicating successful conjugation reactions. A shift in the molecular weights of conjugated products was also confirmed by GPC, demonstrating an 81% conjugation of the PEG-GPSG-PEG.

In vitro degradation of peptides and PEG-GPSG-PEG hydrogels

Mass spectrometry (MALDI-ToF) following incubation of the peptides GPMGPSGPWGK and GMPSGGPPWGK in cathepsin K or buffer, revealed peaks at predicted molecular weights (predicted: 1070.39 Da; actual: 1091.23 Da) when incubated in NaOAc buffer. When incubated in cathepsin K, the peak at 1091.23 Da disappeared for the sequence GPMGPSGPWGK and predicted degradation peaks appeared at 280.26, 324.38, and 379.39 Da. When the scrambled sequence GMPSGGPPWGK was incubated in cathepsin K, there was no change to the spectrum.

The tryptophan incorporated in the GGGMGPSGPWGGK peptide allowed detection of enzymatic cleavage of the PEG-GPSG-PEG hydrogels by monitoring the release of tryptophan into solution. After incubation in different enzyme

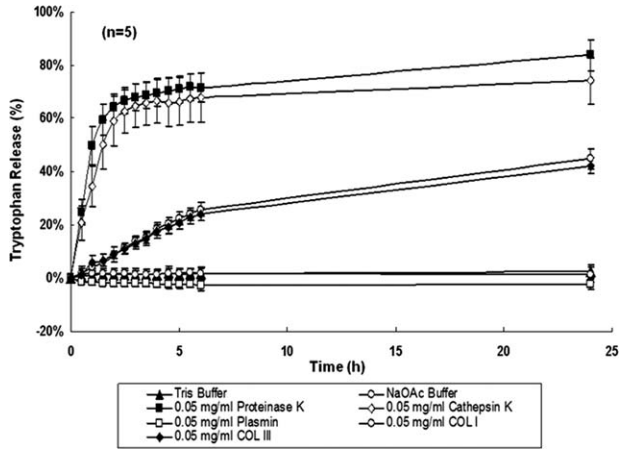

FIGURE 2. Degradation profiles of cathepsin K-sensitive GPSG hydrogels. Hydrogel droplets (3 μL) were polymerized in micro-cuvettes and swelled overnight with 250 μL of TBS buffer. Each hydrogel was incubated in buffer or enzyme solution at 0.05 mg/mL at 37°C. UV absorbance at 280 nm was measured over 24 h to monitor tryptophan release corresponding to the degradation of the GPSP hydrogels.

solutions for 24 h, hydrogels in cathepsin K and proteinase K solutions had similar degradation profiles, both indicating a rapid tryptophan concentration increase within the first hour and reaching about 80% release of total tryptophan at 24 h (Fig. 2). No degradation was observed when hydrogels were incubated in TBS buffer, NaOAc buffer, or plasmin. Hydrogels incubated in nonspecific collagenase I and collagenase III solutions also released 40% of incorporated tryptophan after a 24-h incubation.

Differentiation of RAW264.7

RAW264.7 cells stained for TRAP activity were all negative prior to incubation with RANKL and all positive afterwards. Although all RANKL exposed RAW264.7 cells stained TRAP positive, not all of these cells fused into multinuclear cells [Fig. 3(A)]. After separation by serum gradient, the top fraction of the gradient contained most of the mononuclear cells. The middle fraction of the gradient contained mixed groups of mononuclear and multinuclear cells. The majority of cells in the bottom fraction were multinuclear, containing a very small portion of mononuclear cells [Fig. 3(B–D)]. The multinuclear cells collected in the bottom fraction also stained TRAP positive, which indicated that they were differentiated multinuclear osteoclasts.

Comparison of surface resorption pits on cathepsin K-sensitive hydrogels and bone slices

After incubating with differentiated RAW264.7 cells for 48 h, the surfaces of both the hydrogels and bone slices revealed similar resorption pits (Fig. 4). The resorption pits on the hydrogel were smaller and greater in number than

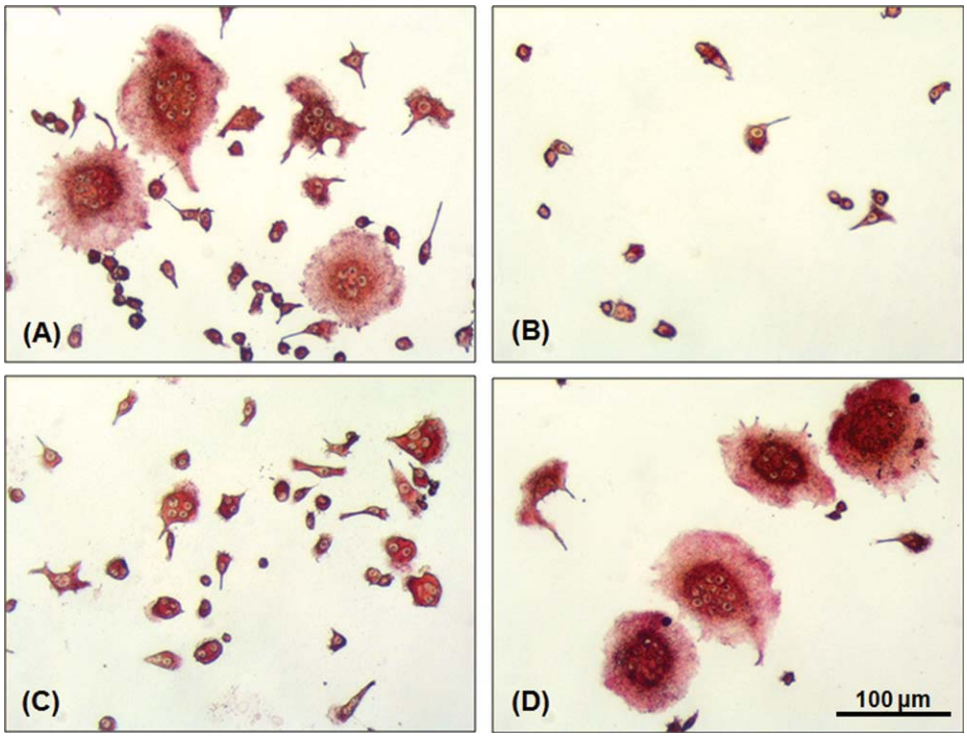

FIGURE 3. Isolated TRAP-positive dRAW264.7 osteoclasts by serum gradient. After differentiation in medium containing 30 ng/mL RANKL for 4 days, dRAW264.7 cells were combined with mono- and multi-nuclear cells [Fig. 3(A)]. After separation by serum gradient, the top fraction contained most of the mononuclear cells. The middle fraction of the gradient contained mixed groups of mononuclear and multinuclear cells. The majority of cells in the bottom fraction were multinuclear cells, which contained a very small portion of mononuclear cells [Fig. 3(B–D)]. The multinuclear cells collected in the bottom fraction were also stained TRAP positive, which indicated that they were activated osteoclasts. The bottom fraction of TRAP+ dRAW 264.7 osteoclasts was then used for hydrogel degradation studies.

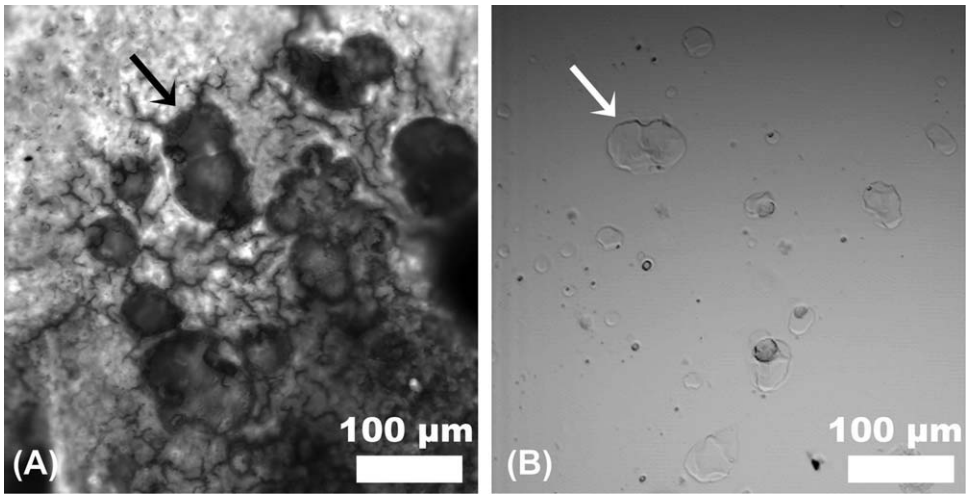

FIGURE 4. Comparison of resorption pits on both (A) bone slices and (B) GPSG hydrogels seeded with dRAW264.7 osteoclasts. Cells were seeded and cultured for 48 h. Cells were detached with 20 m*M* EDTA and images of hydrogel and bone slice surfaces were obtained on a LSM LIVE 5 confocal microscope. Similar pit features were observed on both bone slices and hydrogels. Although the pits on the hydrogel are smaller and also outnumbered the pits on the bone slices, both hydrogels and bone slices have a similar percentage of total resorption area.

those on the bone. Despite the differences in size and number, the morphology of the pits was indistinguishable. Both hydrogel and bone slice surfaces were resorbed at the same order of magnitude (18,497.94 ± 65.03 μm^2 and 25,495.12 ± 24.58 μm^2), with similar percentages of total resorbed areas of 9.56% ± 0.03% and 13.17% ± 0.01%, respectively.

DIC images of cathepsin K-sensitive hydrogel surfaces seeded with dMC3T3-E1 and dRAW264.7

No features were detected on hydrogel surfaces seeded with dMC3T3-E1 osteoblasts [Fig. 5(A)]. On hydrogel surfaces seeded with dRAW264.7 osteoclasts, several features were observed after cells were detached [Fig. 5(B)]. The intensity profile of the DIC image [Fig. 5(D)] suggests that the features on the hydrogels were depressions.

Three dimensional image reconstruction of dRAW264.7 cells on the surface of cathepsin K-sensitive hydrogels

dRAW264.7 cells stained with DAPI and rhodamine phalloidin showed multinuclear, polarized cells on the hydrogel surface [Fig. 6(A); Supporting Information A video]. A sealing ring of F-actin and multiple nuclei were clearly observed [Fig. 6(B)]. Within the hydrogel surface beneath an osteoclast, a decrease in the hydrogel's fluorescent signal was observed [Fig. 6(C)]. Three dimensional volume reconstructions of z-stack images further illustrate this fluorescent signal loss by showing it as a hole in the hydrogel through which the cell can be visualized [Fig. 6(D–F)]. This signal loss is indicative of activity by the differentiated RAW264.7 osteoclasts, degrading the underlying hydrogel and creating a characteristic resorption pit, resulting in the fluorescent intensity loss. No signal loss was observed on the hydrogels seeded with dMC3T3-E1 cells (Fig. 7).

DISCUSSION

In order to design an osteoclast degradable material, a cathepsin K-sensitive peptide derived from a collagen (α-1) fragment[9] was examined for its capability to provide enzyme-degradable cleavage sites within PEG hydrogels. During the synthesis of the cathepsin K-sensitive, PEG polymer, we employed a method shown to result in selectively high yields of the desired acryloyl-PEG-GPSG-PEG-acryloyl.[10] Although unconjugated peptides and double conjugation in the form of GPSG-PEG-GPSG are possible, Miller et al. previously demonstrated that such species, which are initially physically entrapped within hydrogel, diffuse out during equilibrium swelling because they are not covalently bound.[13] Successfully conjugated acryloyl-PEG-GPSG-PEG-acryloyl also generates a distinct molecular weight shift, which makes dialysis a valid option for purification. Our GPC results confirmed this shift, corresponding to a conjugation yield of 81%.

The sensitivity of our peptide to cathepsin K was first evaluated by incubating GPM↓GPS↓GPWGK (predicted: 1070.39 Da; actual: 1091.23 Da) with cathepsin K, with the reported cleavage sites indicated by arrows. Our MALDI-ToF results showed the molecular weights of GPM (predicted: 303.38 Da; actual: 324.38 Da) and GPS (predicted: 259.26 Da; actual: 283.05 Da), confirming these cleavage sites and demonstrating the peptide's sensitivity to cathepsin K. Furthermore, our MALDI-ToF results revealed the molecular weight of the peptide GPW (predicted: 358.39 Da; actual: 381.06 Da), indicating that in addition to the reported cleavage site between M–G and P–S, cathepsin K can also recognize and cleave the peptide between tryptophan (W) and G. Hence our peptide contains three cathepsin K cleavage sites: GPM↓GPS↓GPW↓GK. A scrambled version of the peptide GMPSGGPPWGK, in which the cathepsin K recognition site G-P-X-G (X represents serine, methionine, arginine (R), glutamine (Q)[9] or tryptophan) was disturbed did not degrade in the presence of cathepsin K, indicating the specificity of the enzyme for our sequence.

After establishing the specificity of cathepsin K for our peptide, we altered the sequence to GGGMGPS↓GPW↓GGK in order to permit conjugation with acryloyl-PEG-SMC while

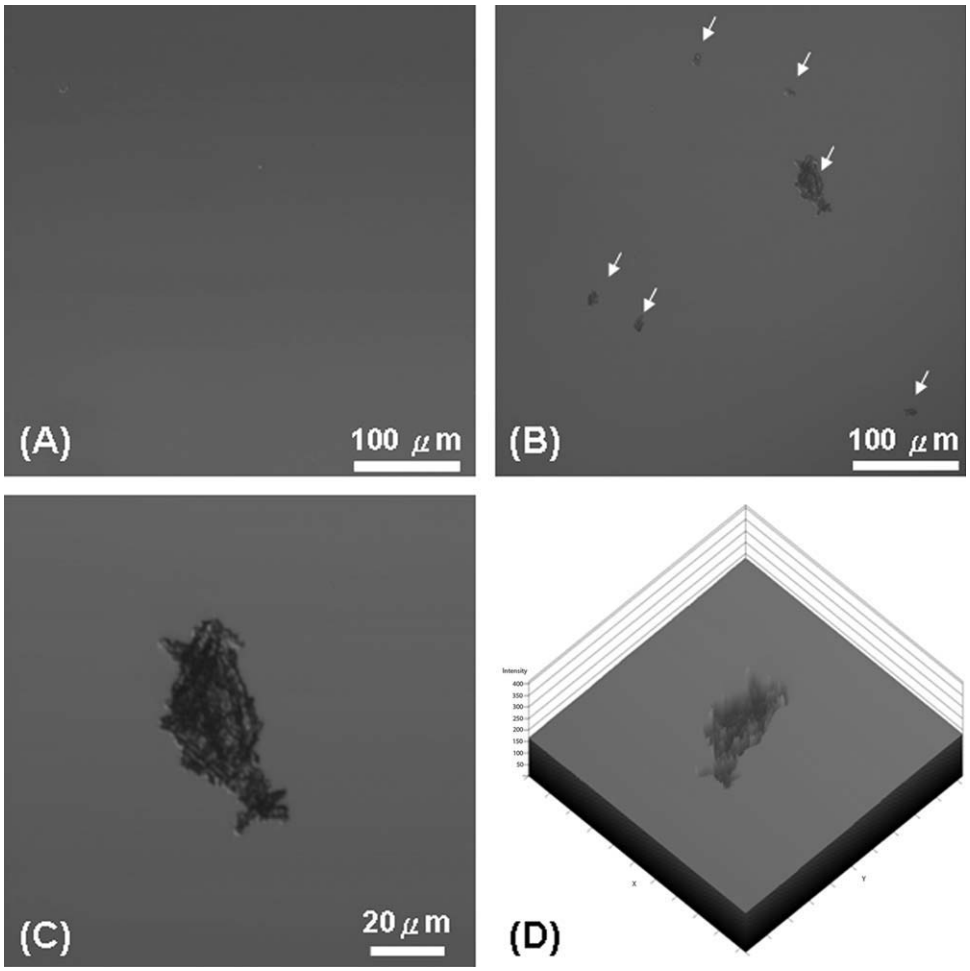

FIGURE 5. Differential interference contrast (DIC) images of GPSG hydrogel surfaces seeded with (A) dMC3T3-E1 osteoblasts and (B) dRAW264.7 osteoclasts. Cells were seeded on the hydrogels and cultured for 48 h. Cells were detached with 20 m*M* EDTA and DIC images were obtained on a LSM LIVE 5 confocal microscope. No features were observed on gel surfaces seeded with osteoblasts (A). On the gel surface seeded with osteoclasts (B), several features can be identified after cells were detached. (C) and (D) show an enlarged image and an intensity profile of the feature, which suggests that the features on the surface were depressions.

avoiding steric hindrance with the enzyme. In order to evaluate the sensitivity of cathepsin K for our hydrogel, we incubated the hydrogel before and after polymerization with cathepsin K, proteinase K, collagenases, and buffers. Proteinase K is one of the most active endopeptidases reported. It is a nonspecific serine protease extracted from fungus *Tritirachium album*[14] and was selected as a positive control. Proteinase K does not exhibit pronounced cleavage specificity and its predominant cleavage sites are peptide bonds adjacent to carboxyl groups of aliphatic, aromatic, or hydrophobic amino acids. Simply, it cleaves proteins and peptides at A↓B, where A is an aliphatic, aromatic or hydrophobic amino acid and B is any amino acid. According to the ExPASy proteomics PeptideCutter tool (Swiss Institute of Bioinformatics), proteinase K cleaves our peptide sequence at the carboxyl side of the tryptophan (GGGMGPSGPW↓GGK), which is a hydrophobic and aromatic residue. Our results showed that cathepsin K degraded the PEG-GPSG-PEG hydrogel at the same rate and amount as proteinase K, indicating that cathepsin K had a high sensitivity for our polymer.

In order to demonstrate the specificity of our polymer for degradation by cathepsin K, we selected collagenases type I, type III, and plasmin as negative controls. These proteases are specific to other sequences and, as expected, did not degrade the hydrogel to the same degree as proteinase K or cathepsin K. The collagenases only showed a moderate effect on our collagen-derived GPSG sequence, while plasmin was unable to degrade the peptide at all. Plasmin is an important serine protease present in blood. It plays a significant role during wound healing processes and clot dissolution.[15] The fact that plasmin has no sensitivity for our GPSG hydrogel poses an important advantage for future clinical applications, ensuring the hydrogel will persist without undergoing nonspecific degradation mediated by wound healing processes.

After we established cathepsin K's sensitivity and specificity for our hydrogel, we demonstrated the capacity of our polymer to undergo osteoclast-specific degradation. When degrading bone, osteoclasts release hydrochloric acid to degrade the mineral component and collagenases and cathepsins

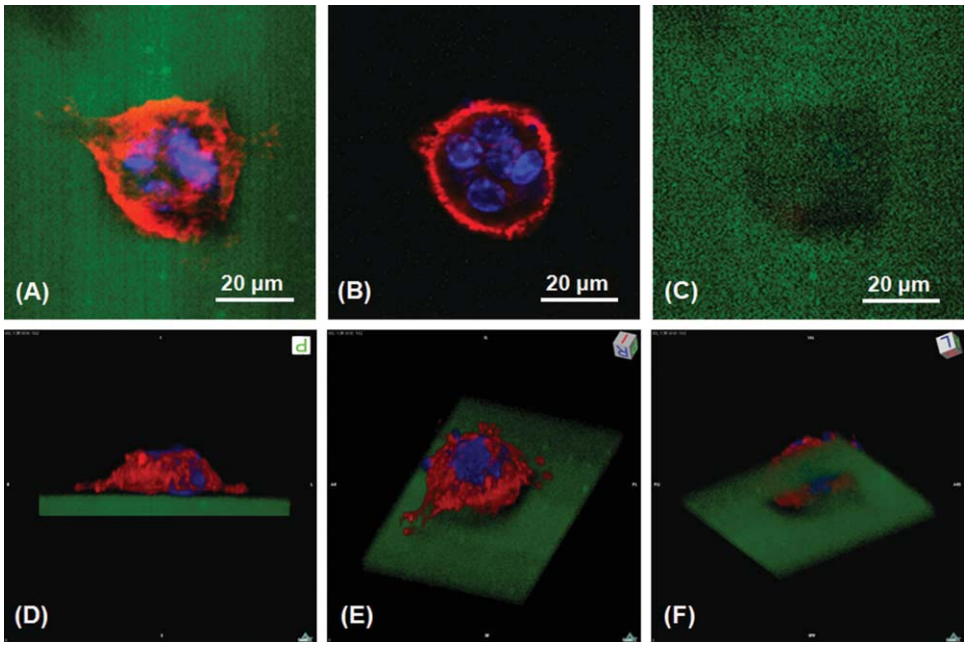

FIGURE 6. Three-dimensional fluorescent image reconstruction of an active osteoclast on the GPSG hydrogel surface. The GPSG hydrogel was labeled with Alexafluor 680 fluorophore (green), which is conjugated to the acryloyl-PEG-RGDS and incorporated into the hydrogel by photopolymerization. The cells were fixed and permeabilized before staining the nuclei with DAPI (blue) and F-actin by rhodamine phalloidin (red) 48 h after seeding. (A) Composed z-stack images of the osteoclast and hydrogel. (B) Sealing ring and multiple nuclei of the osteoclast. (C) The reduced fluorescent signal in the GPSG hydrogel marks the site of an osteoclast resorption pit. These pits, or resorption lacunae, are an extracellular space between the osteoclast ruffled border membrane and the hydrogel, which is sealed from the extracellular fluid by the sealing zone. (D–F) Z-stack Images were reconstructed using a volume rendering algorithm. (D) Side view shows the dome shape of the cell sitting above its resorption lacuna, indicating the polarization of an active osteoclast. (E) Orthogonal view of active osteoclast shown from above. (F) The orthogonal view from below shows a view of the osteoclast through the hole it has degraded in the hydrogel. This resorption site is located beneath the osteoclast, which can be observed in the loss of the fluorescent intensity of Alexafluor 680. The resorption lacuna on the hydrogel surface can be clearly seen from different angles, suggesting that the GPSG hydrogel has been degraded by cathepsin K secreted by osteoclasts.

to degrade the collagenous bone matrix. After a cycle of resorption, the osteoclast undergoes apoptosis, thus normal degradation proceeds as a sustained series of pitting processes. Our results showed such pitting with differentiated RAW267.4 osteoclasts on both bone and our hydrogel. Although the hydrogel resorption pits were smaller and greater in number than those on the bone, similar differences in osteoclast resorption pit number and size on various biomaterials were attributed to degradation-induced calcium release,[16] which is thought to regulate osteoclastic resorption.[17] Since our hydrogel does not contain calcium, it does not stimulate this response. Nevertheless, the identical morphology of the pits on both surfaces and the comparable area resorbed indicate that osteoclasts were indeed capable of resorbing our PEG-GPSG-PEG hydrogel.

In summary, results of this study demonstrate our ability to synthesize an osteoclast degradable hydrogel. By incorporating the collagen I (α-1) peptide fragment, we have developed a synthetic polymer with a high sensitivity and specificity for cathepsin K. Enzyme degradation experiments establish that both the peptide fragment and polymerized hydrogel are degradable by cathepsin K, whereas nonspecific collagenases only have a moderate effect. Cell culture experiments demonstrated that osteoclasts are capable of binding to and degrading an RGDS-modified version of this hydrogel. When seeded with osteoblasts or osteoclasts, these hydrogels showed evidence of degradation only on surfaces seeded with osteoclasts, which revealed characteristic resorption pits, further demonstrating that degradation of the polymer is both enzyme and cell specific. In particular, our hydrogel is specific to the enzymes and cells with key roles in bone resorption.

We have previously demonstrated success forming heterotopic bone using genetically modified cells encapsulated in PEG hydrogels.[18] These cells were transduced with an adenoviral vector to express bone morphogenetic protein, type 2 (BMP-2). The encapsulation with PEG was an improvement over directly injecting these cells because it enables the use of nonautologous cells in immune competent animals.[19] Despite the success in bone formation, bone did not form where the hydrogel was present. Because the modified cells need immunoprotection only for the duration of bone formation, degradation of the hydrogel after the cells have served their purpose would be beneficial. Although there exist hydrolytically degradable hydrogel systems, our cathepsin K-degradable polymer would be an improvement over such systems because degradation would be timed to the arrival of osteoclasts, and would proceed during the remodeling process of the newly formed bone. Hydrolytically-degradable systems degrade at a set rate,

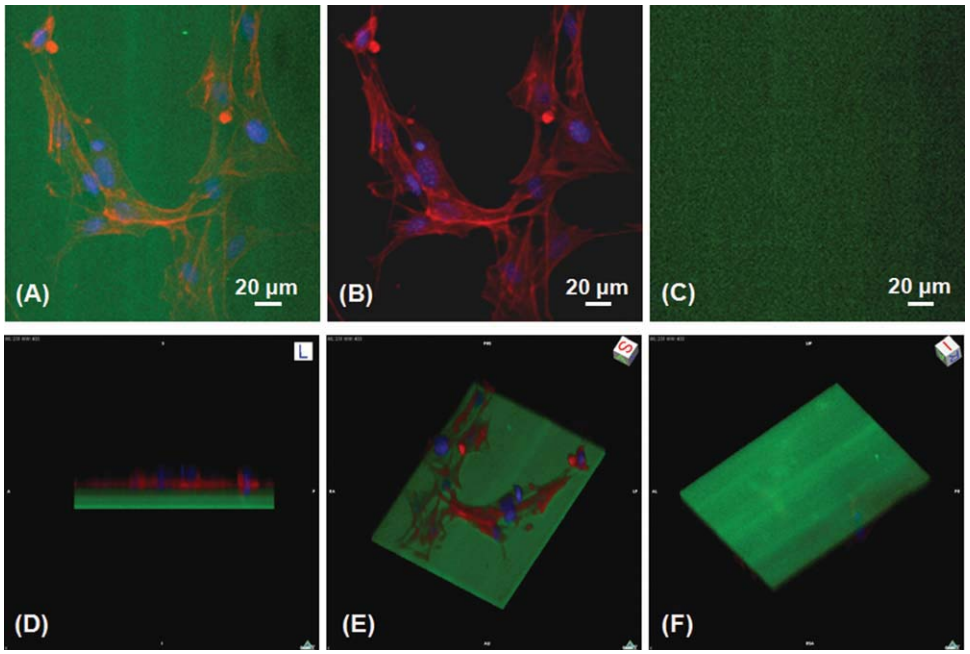

FIGURE 7. Three-dimensional fluorescent image reconstruction of osteoblasts on the GPSG hydrogel surface. The GPSG hydrogel was labeled with Alexafluor 680 fluorophore (green), which is conjugated with the acryloyl-PEG-RGDS and incorporated into the hydrogel by photo-polymerization. The cells were fixed and permeabilized before staining the nuclei with DAPI (blue) and F-actin by rhodamine phalloidin (red) 48 h after seeding. (A) Composed z-stack images of the osteoblasts and hydrogel. (B) Osteoblasts shown without the hydrogel. (C) GPSG hydrogel shown without the osteoblasts shows no decrease in fluorescent signal beneath the osteoblasts. Z-stack Images were reconstructed using a volume renderings algorithm and presented from (D) side view, (E) orthogonal view from above, and (F) from below.

purely dependent upon water uptake. Because bone formation proceeds differently between each individual, a set rate that might be ideal in one animal or patient may not be appropriate for another. Thus, the rate of degradation should be set by the rate of bone remodeling. Cell-mediated degradation is useful in any scenario where the presence of the hydrogel is needed until the host tissue has replaced it. When cell types other than osteoclasts are targeted for material degradation, one can easily change the peptide sequence in the polymer backbone to achieve sensitivity to other proteolytic enzymes. This approach could improve the design of tissue engineering scaffolds, wound dressings, and other biomaterial devices.

CONCLUSIONS

In summary, we have successfully used PEG hydrogels as a model system to demonstrate a new strategy to initiate biomaterial degradation through a specific cellular response. We developed a PEG hydrogel system with a cathepsin K-sensitive peptide sequence, GPSG, incorporated into the polymer backbone. This hydrogel system can be gradually degraded with cathepsin K secreted by osteoclasts during bone resorption processes. In the future, this strategy can be applied to different biomaterials to improve their performance in orthopedic applications.

ACKNOWLEDGMENT

The authors thank Melissa McHale for her assistance in editing this work.

REFERENCES

1. Price CT, Connolly JF, Carantzas AC, Ilyas I. Comparison of bone grafts for posterior spinal fusion in adolescent idiopathic scoliosis. Spine (Phila Pa 1976). 2003;28:793–798.
2. Goldberg VM. Selection of bone grafts for revision total hip arthroplasty. Clin Orthop Relat Res 2000:68–76.
3. Nishida J, Shimamura T. Methods of reconstruction for bone defect after tumor excision: A review of alternatives. Med Sci Monit 2008;14:RA107–RA113.
4. Malizos KN, Zalavras CG, Soucacos PN, Beris AE, Urbaniak JR. Free vascularized fibular grafts for reconstruction of skeletal defects. J Am Acad Orthop Surg 2004;12:360–369.
5. Cornell CN. Osteobiologics. Bull Hosp Jt Dis 2004;62:13–17.
6. Hill PA. Bone remodelling. Br J Orthod 1998;25:101–107.
7. Vaananen HK, Zhao H, Mulari M, Halleen JM. The cell biology of osteoclast function. J Cell Sci 2000;113(Part 3):377–381.
8. Lecaille F, Bromme D, Lalmanach G. Biochemical properties and regulation of cathepsin K activity. Biochimie 2008;90:208–226.
9. Nosaka AY, Kanaori K, Teno N, Togame H, Inaoka T, Takai M, Kokubo T. Conformational studies on the specific cleavage site of Type I collagen (alpha-1) fragment (157–192) by cathepsins K and L by proton NMR spectroscopy. Bioorg Med Chem 1999;7:375–379.
10. Bouzide A, Sauve G. Silver (I) oxide mediated highly selective monotosylation of symmetrical diols. Application to the synthesis of polysubstituted cyclic ethers. Org Lett 2002;4:2329–2332.
11. Hahn MS, Taite LJ, Moon JJ, Rowland MC, Ruffino KA, West JL. Photolithographic patterning of polyethylene glycol hydrogels. Biomaterials 2006;27:2519–2524.
12. Collin-Osdoby P, Yu X, Zheng H, Osdoby P. RANKL-mediated osteoclast formation from murine RAW 264.7 cells. Methods Mol Med 2003;80:153–166.
13. Miller JS, Shen CJ, Legant WR, Baranski JD, Blakely BL, Chen CS. Bioactive hydrogels made from step-growth derived PEG-peptide macromers. Biomaterials 2010;31:3736–3743.
14. Ebeling W, Hennrich N, Klockow M, Metz H, Orth HD, Lang H. Proteinase K from Tritirachium album limber. Eur J Biochem 1974;47:91–97.

15. Li WY, Chong SS, Huang EY, Tuan TL. Plasminogen activator/plasmin system: A major player in wound healing? Wound Repair Regen 2003;11:239–247.
16. Redey SA, Razzouk S, Rey C, Bernache-Assollant D, Leroy G, Nardin M, Cournot G. Osteoclast adhesion and activity on synthetic hydroxyapatite, carbonated hydroxyapatite, and natural calcium carbonate: Relationship to surface energies. J Biomed Mater Res A 1999;45:140–147.
17. Kameda T, Mano H, Yamada Y, Takai H, Amizuka N, Kobori M, Izumi N, Kawashima H, Ozawa H, Ikeda K. Calcium-sensing receptor in mature osteoclasts, which are bone resorbing cells. Biochem Biophys Res Commun 1998;245:419–422.
18. Bikram M, Fouletier-Dilling C, Hipp J, Gannon F, Davis A, Olmsted-Davis E, West J. Endochondral bone formation from hydrogel carriers loaded with BMP2-transduced cells. Annals Biomed Eng 2007;35:796–807.
19. Cruise GM, Hegre OD, Lamberti FV, Hager SR, Hill R, Scharp DS, Hubbell JA. In vitro and in vivo performance of porcine islets encapsulated in interfacially photopolymerized poly (ethylene glycol) diacrylate membranes. Cell Transplant 1999;8:293–306.